14th Australasian Fluid Mechanics Conference
Adelaide University, Adelaide, Australia
10-14 December 2001

Visualization of Turbulent Structure in the Drag-Reducing Flow of Aqueous Surfactant Solution

M. Itoh[1] and Y. Kurokawa[1]

[1]Department of Mechanical Engineering
Nagoya Institute of Technology, Nagoya, 466-8555 JAPAN

Abstract

Turbulent structure in the two-dimensional channel flow of drag-reducing surfactant solution is investigated using hydrogen-bubble technique. The visual observations are focussed on the coherent motions in the near-wall region; i.e., ejections and quasi-streamwise vortices. It is revealed that the ejections of near-wall fluid are suppressed in the drag-reducing flows. The ejection could not be observed when 'turbulence reduction – drag' (TRD) is larger than 75%, where TRD is defined using the friction difference between laminar and turbulent flows (Gasljevic and Matthys [2]). It is found that quasi-streamwise vortices exist even at large TRD above 80%. The average position of the quasi-streamwise vortex centre becomes more distant from the wall as TRD increases.

Introduction

It is well known that some kinds of surfactant solution cause a remarkable drag reduction in turbulent flows. Many investigations have been conducted concerning this problem [3,12]. The measurements using LDV (laser Doppler velocimetry) show that the Reynolds shear stress is close to zero in surfactant solutions with large drag reduction [3,11]. Warholic et al. [11] conjectured that the quasi-streamwise vortices do not exist near the wall under maximum drag reduction. In our previous experiment [5], we visualized low-speed streaks in the two-dimensional channel flow of drag-reducing surfactant solutions and showed that the low-speed streaks exist even at large drag reduction. It was also revealed that, in the drag-reducing flows, the mean streak spacing reaches a minimum at some distance from the wall and the streaks decrease rapidly with approaching the wall. In order to interpret these experimental evidences, the coherent motions near the wall (ejections and quasi-streamwise vortex motions) are visualized in the present work. Hydrogen-bubble technique is widely used to visualize the coherent motions.

Experimental Apparatus and Procedure

The experimental apparatus used in this work is the same with the one used before [4]. The two-dimensional channel is made of acrylic plates and the dimensions are the width W = 40 mm, the height H = 400 mm and the length L = 4 m. The pressure drops were measured from static pressure taps situated at 65W~90W downstream from the channel inlet. The velocity measurements and the visual observations of near-wall turbulent structures were made using the hydrogen-bubble technique [6,9]. Figure 1 shows the details of the measuring section. The wire used for generating hydrogen-bubbles was a 30 μ m stainless-steel wire. A DC pulse generator was used to generate hydrogen-bubbles, and the hydrogen-bubble time-lines or sheets were viewed and recorded using a CCD video camera and a VTR. The individual video frames were converted to a digital array using an image-processing system and then analysed by a microcomputer.

The surfactant system used here consisted of equimolar mixtures of n-cetyltrimethylannmonium chloride with sodium salicylate, which were added pure water that removed ions and impurities from tap water by a water purifier and a 5 μ m dust filter. The concentrations of the mixture (C_{16}TASal) used here were from 75 ppm to 150 ppm by weight.

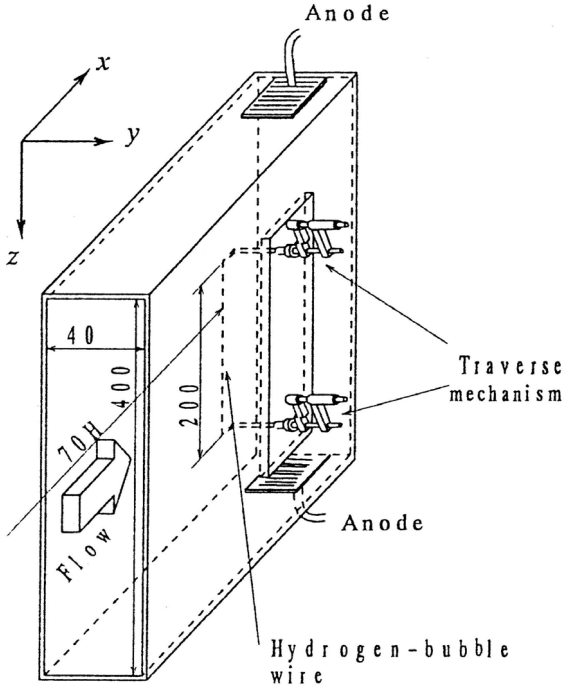

Figure 1. Test section

Experimental Results and Discussion

Pressure drop

Figure 2 shows experimental results for the friction factor λ versus Reynolds number Re. Shown by the solid lines in this figure are the laminar theoretical value

$$\lambda = 1.313 \times 64/\mathrm{Re} \quad (1)$$

and Blasius's equation for Newtonian turbulent flow

$$\lambda = 0.3164\ \mathrm{Re}^{-0.25} \quad (2)$$

along with the maximum drag reduction asymptote for polymer solutions which was found by empirically by Virk [10]

$$1/\sqrt{\lambda} = 9.5 \log(\mathrm{Re}\sqrt{\lambda}) - 19.06 \quad (3)$$

It is noted from the data for 75 ppm surfactant solution that the friction factor for the surfactant solution shows strong temperature dependence. This may be caused by the fact that the length of the rod-like micelle in the solution becomes shorter with the fluid temperature increase [7]. In Fig. 3, we show the parameter 'turbulence reduction – drag' (TRD) defined as follows.

$$TRD = \frac{\lambda_{T0} - \lambda}{\lambda_{T0} - \lambda_{L0}} \quad (4)$$

In Eq. (4), the subscripts 'T0' and 'L0' mean turbulent and laminar flows for the non-drag reducing 'Newtonian' fluid at the same Reynolds number, respectively. This parameter was introduced by Gasljevic and Matthys [2] in place of the usual drag reduction parameter, DR, (which represents the change in friction relative to the level of turbulent friction for a corresponding Newtonian fluid) to improve quantification of the drag reduction phenomena. It can be seen that the values of TRD for 150 ppm solution are so high as 80~90%.

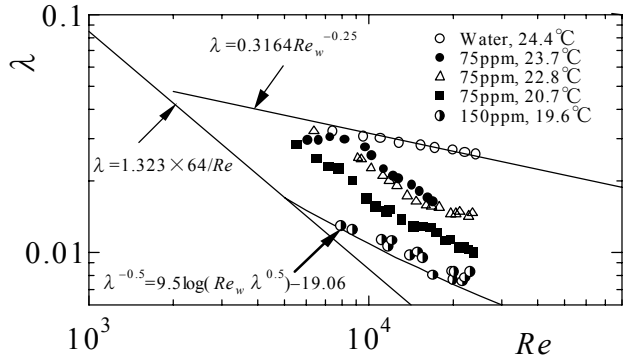

Figure 2. Friction factor

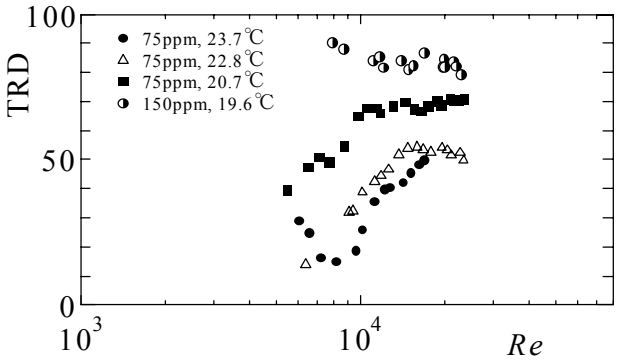

Figure 3. Turbulence reduction-drag

Velocity field

Figure 4 shows the contour plots of velocity for various drag reducing flows at Re = 12,000. The notations y^+ and t^+ are the wall-normal distance and time, respectively, nondimensionalized with wall variables u_τ and ν. With increasing drag reduction, the burst-type motions seem to be strongly suppressed. In Fig. 5(c), only small fluctuations can be seen along individual contour lines near the wall.

The mean velocity profiles are shown in Fig. 5. In the case of TRD = 44%, the velocity profile in the log-law region shows nearly a straight line parallel to the logarithmic distribution for Newtonian fluid.

$$\overline{u^+} = 5.75 \log y^+ + 5.5 \qquad (5)$$

The profile for TRD = 87% is close to the laminar profile shown by a broken line and an S-shaped one as pointed out by several authors[3 ,11]. In the region of y^+>40, the profile exceeds Virk's ultimate profile [10] given by the following equation.

$$\overline{u^+} = 26.9 \log y^+ - 17 \qquad (6)$$

Ejections

In order to investigate the bursting phenomena in detail, we observed the motions of hydrogen-bubble sheet generated by the wire at $y^+ = 15$. A slit light source of width $\Delta z^+ \approx 100$ was used to illuminate the central part of the hydrogen-bubble sheet. Figure 6 shows an example of the visual sequence of an ejection

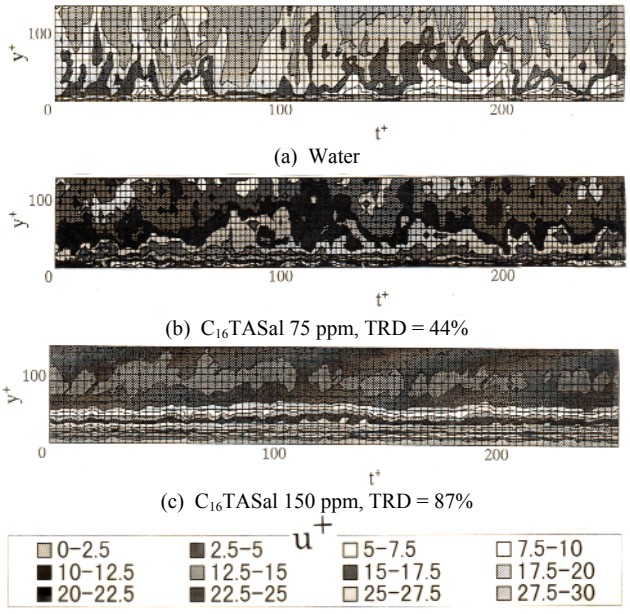

Figure 4. Contour plot of velocity (Re = 12,000)

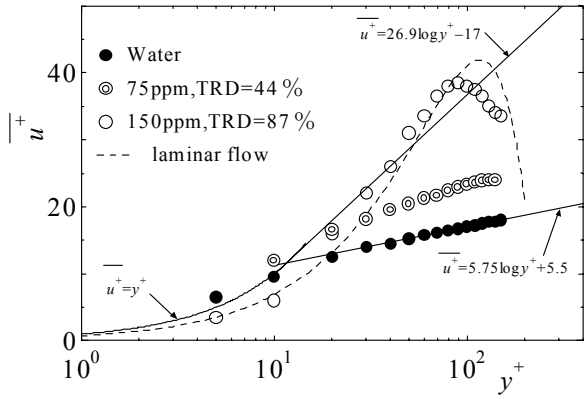

Figure 5. Mean velocity profile (Re = 12,000)

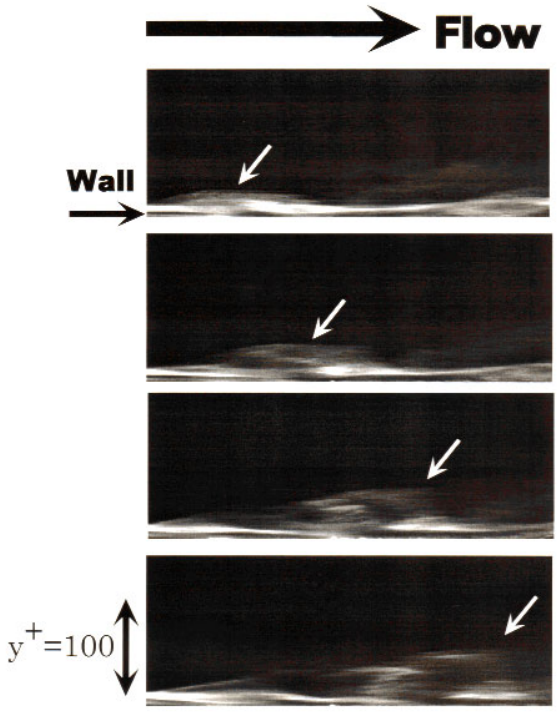

Figure 6. Ejection (Water, Re = 8,000, every 1/10 sec)

event. The arrows in the photographs depict the ejection motion of the near-wall fluid.

Careful analysis of the video sequences was made for various combinations of TRD and Re. Figure 7 shows the maximum outward displacement of the bubble-sheet, $\Delta y^{+}{}_{max}$, within the region Δx^{+}<350 downstream of the bubble-generating wire. It will be known from the figure that the ejection does not occur in the drag-reducing flow of TRD>75%. The strength of ejections was found to be not only dependent on TRD but also on Re.

The averaged period of ejections, $\overline{Te^{+}}$, is shown in Fig. 8. In order to detect the ejections, the following two criteria proposed by Bogard and Tiederman [1] were adopted.

(1) The element of fluid marked by hydrogen-bubbles must originate from the region below $y^{+} = 15$.

(2) An upward movement of at least $\Delta y^{+} = 20$ within a streamwise distance of $\Delta x^{+} = 350$ must occur.

As seen in the figure, $\overline{Te^{+}}$ increases almost linearly with increasing TRD at Re>11,000. It was found that the ejection does hardly occur when TRD was larger than 70%.

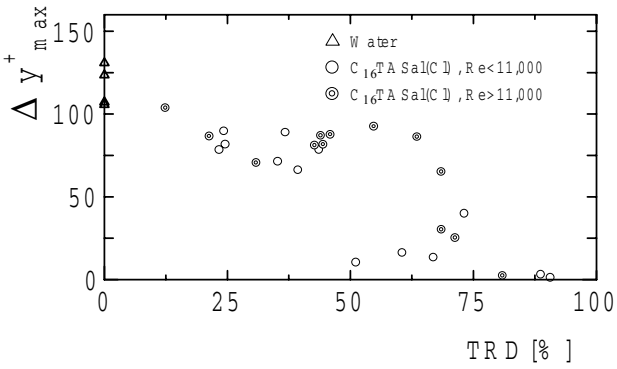

Figure 7. Maximum strength of ejections

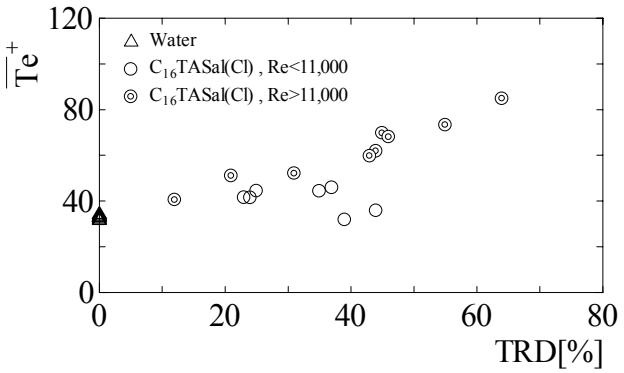

Figure 8. Averaged period of ejections

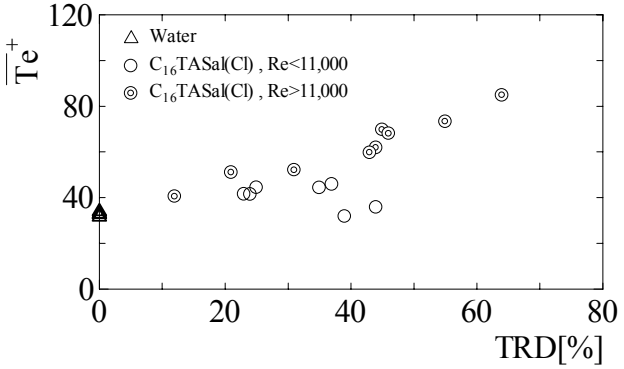

Figure 9. Averaged strength of ejections

Figure 9 shows the variance of the averaged strength of ejections with TRD. The values of $\overline{\Delta y^{+}}$ were obtained by measuring the averaged outward displacement of the hydrogen-bubble sheet within a streamwise distance of $\Delta x^{+} = 350$. It is noticed that the averaged strength of ejections decreases with increasing TRD at lower TRD (<25%) but its dependence on TRD is very weak at higher TRD.

Quasi-streamwise vortices

It is well known that the quasi-streamwise vortices play a dominant role in the near-wall turbulence [8]. Visualization of the quasi-streamwise vortices was done using three-wire hydrogen-bubble probe similar to that used by Smith and Schwartz [9]. All the three wires are to be located parallel to the wall and transverse to the flow direction. Figure 10 shows typical end-view pictures. A slit light of 5 mm thickness was used to illuminate the flow-normal section at 20~25 mm downstream of the bubble-wires. The values of y^{+} shown under each picture are the wall-normal distances of three wires. In the pictures, corrugated white lines imply the existence of streamwise vortices near the wall. In the case of large TRD (Fig.10 (c)), however, the existence of streamwise vortices could not be confirmed in those pictures taken by lighting the flow-normal section near the bubble-wires. Therefore, we observed the end-view of the bubble sheets at further downstream of the bubble-wires.

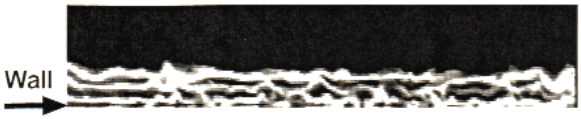

(a) Water, y^{+} = 10, 36, 62

(b) C_{16}TASal 75 ppm, TRD = 34% , y^{+} = 10, 32,55

(c) C_{16}TASal 100 ppm, TRD = 81% , y^{+} = 10, 28, 46

Figure 10. End-view of quasi-streamwise vortices (Re = 10,000)

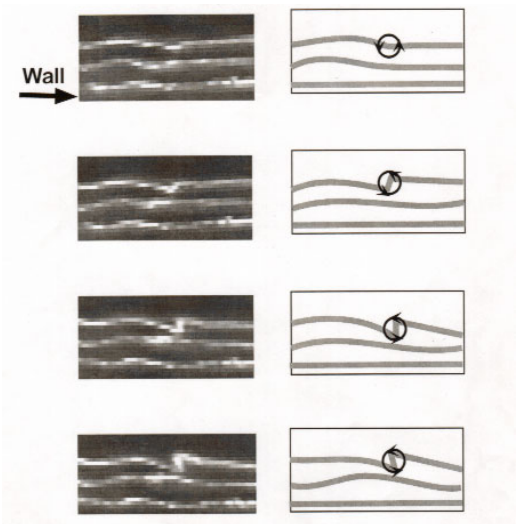

(a) Visualization sequence (b) Sketch showing vortex roll-up

Figure 11. Quasi-streamwise vortex (Re = 10,000 , TRD = 81%)

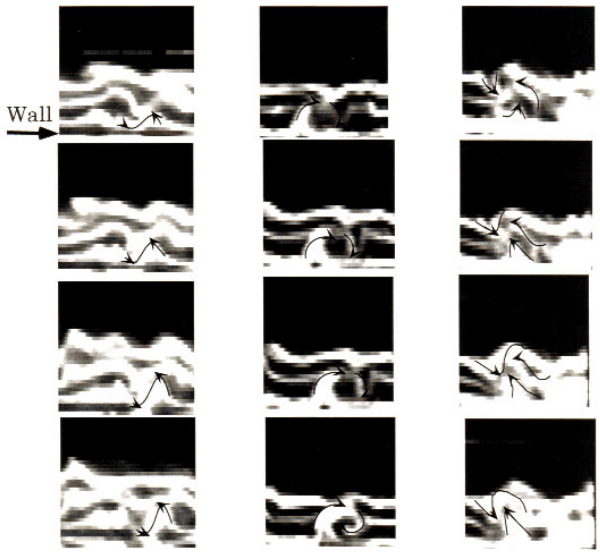

Figure 12. End-view visualization sequence
(Water, Re = 10,000 , every 1/30 sec)

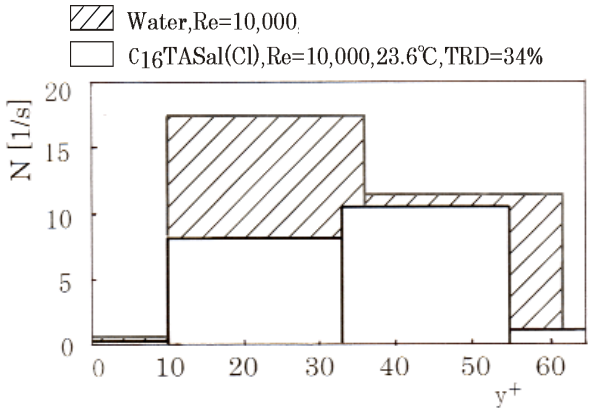

Figure 13. Position of quasi-streamwise vortex centre

Figure 11 shows the end-view visualization sequence obtained for TRD = 81% by lighting the flow-normal section at 50~55 mm downstream of the bubble-wires. As illustrated in Fig. 11 (b), the most upper bubble sheet clearly indicates the streamwise vortex motion. From extensive analysis of VTR images, it may be concluded that, although the strength of the vortices becomes much weaker, the quasi-streamwise vortices do exist even in the flow of high TRD. It is speculated that in the flow of high TRD the quasi-streamwise vortices are so weak that the ejection does not occur.

Figure 12 shows the end-view visualization sequence illustrating the development of streamwise vortex. The movement of the bubble sheets is depicted in each picture. In this manner we estimated the position of the quasi-streamwise vortex centre. The vortices were divided into four groups according their centre positions, i.e. (1) below the bubble wire 1, (2) between the wires 1 and 2, (3) between the wires 2 and 3, and (4) above the wire 3, where the bubble wire was numbered from that nearest to the wall. Figure 13 shows the number of quasi-streamwise vortices observed within the region of spanwise width $\Delta z^+ = 750$. It is clearly demonstrated that, in the drag-reducing flow, the total number of streamwise vortices is smaller and the average vortex centre is more distant from the wall compared with the non-drag reducing flow.

Conclusions

Visualization studies using the hydrogen-bubble technique were made to clarify the turbulent structure of the drag-reducing flow of an aqueous surfactant solution. The results are summarized as follows.

(1) The ejections of near-wall fluid are suppressed in the drag-reducing flows and no ejection could be observed when 'turbulence reduction – drag' (TRD) is larger than 75%.
(2) The quasi-streamwise vortices can exist even when TRD is larger than 80%.
(3) With increasing TRD, the average position of the quasi-streamwise vortex centre becomes more distant from the wall.

Nomenclature

D : equivalent diameter
Re : Reynolds number (= DU/ν)
t : time
TRD : turbulence reduction-drag
U : bulk mean velocity
u : velocity component in the mean flow direction
u_τ : friction velocity
y : wall-normal distance
λ : friction factor
ν : kinematic viscosity
Superscript
$(^+)$: nondimensional value in terms of u_τ and ν

References

[1] Bogard, D. G. and Tiederman, W. G., *Proc. Symposium on Turbulence,* Missouri-Rolla, 1983, 289-302.
[2] Gasljevic, K and Matthys, E. F., *J. Non-Newtonian Fluid. Mech.,* 84, 1999, 123-130.
[3] Gyr, A. and Bewersdorff, H. –W., *Drag Reduction of Turbulent Flows by Additives,* Kluwer Academic, 1995.
[4] Itoh, M., Imao, S. and Tokuda, K., *Trans. JSME,* Ser. B, 61-590, 1995, 3664-3670. (in Japanese)
[5] Itoh, M., Imao, S. and Sugiyama, K., *JSME Int. J.,* Ser. B, 40-4, 1997, 550-557.
[6] Lu, L. J. and Smith, C. R., *J. Fluid Mech.,* 232, 1991, 303-340.
[7] Ohlendorf, D., Interthal, W. and Hoffmann, H., *Rheol. Acta*, 25, 1986, 468-486.
[8] Robinson, S. K., *Ann. Rev. Fluid Mech.,* 23,1992, 601-639.
[9] Smith, C. R. and Schwartz, S. P., *Phys. Fluids,* 26-3, 1983, 641-652.
[10] Virk, P. S., *AIChE J.,* 21-4, 1975,625-656.
[11] Warholic, M. D., Schmidt, G. M. and Hanratty, T. J., *J. Fluid Mech*. 388, 1999, 1-20.
[12] Zakin, J. L., Lu, B. and BewersdorffH. –W., *Reviews in Chemical Engineering,* 14-4(5), 1998, 253-319.